# Revisiting the single-phase flow model for liquid steel ladle stirred by gas

Najib Alia[a,*], Volker John[a,b], Seppo Ollila[c]

[a]*Weierstrass Institute for Applied Analysis and Stochastics (WIAS), Mohrenstraße 39, D-10117 Berlin, Germany*
[b]*Freie Universität, Department of Mathematics and Computer Science, Arnimallee 6, D-14195 Berlin, Germany*
[c]*SSAB Europe Oy, Rautaruukintie 155, FI-92101 Raahe, Finland*

**Abstract**

Ladle stirring is an important step of the steelmaking process to homogenize the temperature and the chemical composition of the liquid steel and to remove inclusions before casting. Gas is injected from the bottom of the bath to induce a turbulent flow of the liquid steel. Multiphase modeling of ladle stirring can become computationally expensive, especially when used within optimal flow control problems. This note focuses therefore on single-phase flow models. It aims at improving the existing models from the literature. Simulations in a 2d axial-symmetrical configuration, as well as in a real 3d laboratory-scale ladle, are performed. The results obtained with the present model are in a relative good agreement with experimental data and suggest that it can be used as an efficient model in optimal flow control problems.

*Keywords:* ladle stirring, CFD, quasi-single phase models, incompressible Navier–Stokes equations

## 1. Introduction

Gas stirring in ladles is a standard practice in the steelmaking industry to refine and homogenize the liquid steel bath before casting. In this process, a noble gas is injected from the bottom of the ladle through generally one or two nozzles fitted with porous plugs. The gas rises by buoyancy through the liquid steel, forms a gas plume, and causes stirring, i.e., a mixing of the bath (Figure 1).

The final aim of our research consists in developing an optimal flow control model to improve the homogenization of the liquid steel by controlling several parameters, e.g., the position of the nozzles and the flow rate of the injected gas. Such a problem requires the repeated solution of the considered process with slightly changing coefficients. Since gradient-free schemes converge generally very slowly, gradient-based optimization algorithms shall be used. In this regard, one has to compute the derivative of the objective functional with respect to the solution of the partial differential equation (PDE). This step can be performed efficiently by solving an adjoint equation. In the case of a time-dependent nonlinear problem, such as ladle stirring, the adjoint equation is backward in time and its coefficients depend on the primal solution.

---

*Corresponding author

*Email addresses:* `alia@wias-berlin.de` (Najib Alia), `john@wias-berlin.de` (Volker John), `seppo.ollila@ssab.com` (Seppo Ollila)
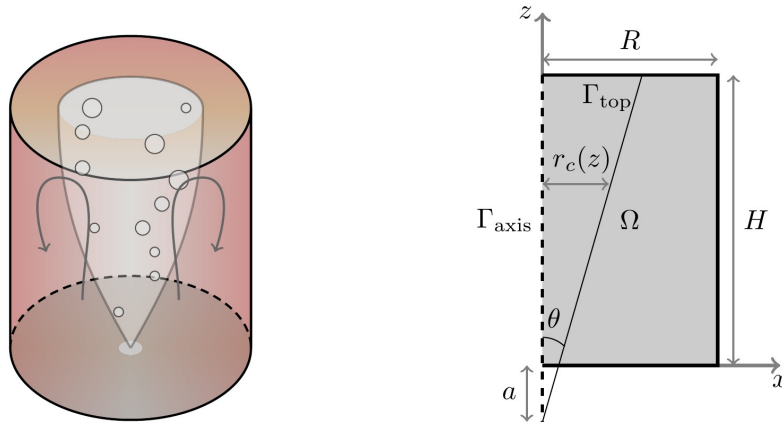
Figure 1: Ladle stirring. Left: Schematic sketch. Right: Axi-symmetric fluid domain.

To keep the cost of the optimal control problem reasonable, reduced order modeling (ROM) is often applied. An example of a modern ROM consists in computing bases for the discrete problems that already possess information about the solution. For time-dependent problems, one performs one simulation with the full model with certain coefficients, stores the so-called snapshots, and computes a basis via a proper orthogonal decomposition (POD), see [1, 2, 3]. This approach is much faster, but its results are somewhat less accurate than with the full model. Furthermore, it becomes complicated for complex mathematical models and their adjoint equations. In addition, it is generally only available in some academic research software. If commercial software is utilized, like in the present note, one has usually only the option to consider from the beginning a mathematical model that is sufficiently efficient. For this reason, single-phase models, which are based on the standard mono-phase incompressible Navier–Stokes equations only ([4]), will be studied here, instead of two-phase gas-liquid flow models. The goal of this note consists in defining an appropriate model which can be used in the simulation of optimal flow control problems.

In the literature, the so-called 'quasi-single phase models' are based on the main assumption that the gas fraction $\alpha$ in the fluid domain is known. Debroy et al. [5], Grévet et al. [6], and Sahai and Guthrie [7] were among the first to perform such numerical simulations on gas-stirred cylindrical ladles with one central nozzle. They applied a conical plume geometry and three slightly different formulas for $\alpha$. In [7], the model additionally uses a non-homogeneous Dirichlet boundary condition on the central vertical axis. Later, Balaji and Mazumdar [8] adapted the existing formulas to propose a fourth variant of $\alpha$, and obtained a better agreement of the numerical results with experimental data. These findings were summarized by Mazumdar and Evans in [9]. In parallel to these works, Woo et al. [10] developed empirical formulas for $\alpha$ based on experimental measurements and obtained better numerical results than in [5] and [6]. Single-phase modeling for bubbles columns was also applied for chemical applications by Bernard et al. [11]. The authors applied a formula similar to [7], except that they included a height correction factor to take into account the volumetric

Table 1: Summary of the studies based on 'quasi-single phase' models.

| Ref. | Year | Model based on | Object of the study |
|---|---|---|---|
| [4] | 1995 | [5, 6, 7, 8, 10][*] | Review of existing 'quasi-single phase' models |
| [5] | 1978 | [5] | Definition for $\alpha$ and application in axi-symmetric ladles |
| [6] | 1982 | [6] | New definition for $\alpha$ |
| [7] | 1982 | [7] | New definition for $\alpha$ in combination with vertical boundary velocity |
| [8] | 1991 | [8, 6, 7] | New definition and comparison of $\alpha$ |
| [9] | 2010 | [8] | - |
| [10] | 1990 | [10, 5, 7] | New definition and comparison of $\alpha$ |
| [12] | 1992 | [8][*] | Application on mass transfer rates |
| [13] | 2004 | [7][*] | Study of thermal stratification |
| [14] | 2001 | [10][*] | Application on temperature and heat transfer |
| [15] | 1996 | [10] | Effect of geometry and nozzle position on mixing time |
| [16] | 2001 | [8] | Effect of geometry and nozzle position on the circulation rate |
| [17] | 1994 | [8][*] | Comparison with Euler-Euler and Euler-Lagrange |
| [18] | 1995 | [8][*] | Comparison with Euler-Euler models |

[*] With minor changes in comparison to original reference.

expansion of the rising gas bubbles. Table 1 summarizes the literature dealing with 'single phase' models.

All single-phase models found several applications, such as the numerical study of mass and heat transfer phenomena ([12, 13, 14]), the improvement of stirring by changing ladle geometry and nozzle positions ([15, 16]), or the comparison with two-phase flow models ([17, 18]). It should be noted that this simplified approach presents some major and known limitations in comparison to state-of-the-art multiphase models, in terms of physical relevance. For example, the prescription of an empirical gas fraction does not include bubbles' wandering effects ([19]). However, as explained earlier, our main reason for using such simplified models is to investigate optimal flow control problems without being limited by computational resources.

Table 2: List of main notations.

| Symbol | Description | Formula | Value | Unit |
|---|---|---|---|---|
| $H$ | Ladle height | - | 0.6 | m |
| $R$ | Ladle radius | - | 0.3 | m |
| $\theta$ | Apex of the conical plume | - | 10 | deg |
| $a$ | Origin of the conical plume | - | 0.08 | m |
| $Q$ | Gas flow rate | - | $2.167 \; 10^{-4}$ (=13) | $\mathrm{m^3/s}$ ($\mathrm{l/min}$) |
| $U_P$ | Plume velocity [21] | $4.4 \dfrac{Q^{1/3}H^{1/4}}{R^{1/4}}$ | - | $\mathrm{m/s}$ |
| $U_S$ | Slip velocity | - | 0.4 | $\mathrm{m/s}$ |
| $r_c(z)$ | Plume radius at height $z$ | $\tan(\theta)\,(z+a)$ | - | m |
| $r_{\mathrm{av}}$ | Average plume radius | $\frac{1}{2}\left(\tan(\theta)\,(2a+H)\right)$ | 0.067 | m |
| $\alpha'_1$ | Gas fraction [7] | $\dfrac{Q}{\pi r_{\mathrm{av}}^2 U_P}$ | - | 1 |
| $\alpha'_2(z)$ | Gas fraction [8] | $\dfrac{Q-\pi r_c^2(z)\alpha'_2(1-\alpha'_2)U_S}{\pi r_c^2(z)U_P}$ | - | 1 |
| $\rho_l$ | Liquid density | - | 1000 | $\mathrm{kg/m^3}$ |
| $\rho_g$ | Gas density | - | 1 | $\mathrm{kg/m^3}$ |
| $\mu$ | Liquid dynamic viscosity | - | $10^{-3}$ | $\mathrm{kg/m.s}$ |
| $\Omega$ | Fluid domain | - | - | - |
| $\Gamma_{\mathrm{top}}$ | Top boundary | - | - | - |
| $\Gamma_{\mathrm{axis}}$ | Left boundary | - | - | - |
| $\boldsymbol{u}$ | Velocity field | - | - | $\mathrm{m/s}$ |
| $p$ | Pressure field | - | - | Pa |
| $\mathbb{S}$ | Stress tensor | $2\mu\mathbb{D}(\boldsymbol{u})+p\mathbb{I}$ | - | $\mathrm{N/m^2}$ |
| $\mathbb{D}$ | Velocity deformation tensor | $\mathbb{D}=\dfrac{\nabla\boldsymbol{u}+(\nabla\boldsymbol{u})^T}{2}$ | - | $\mathrm{1/s}$ |
| $T_{\mathrm{end}}$ | End time | - | - | s |

This note re-visits the single-phase model for ladle stirring with the following contributions:

- clarify the differences between the main formulas for $\alpha$ using a 2d axial-symmetrical configuration,

- and validate a simplified model in 3d on a recent laboratory-scale water ladle experiment [20].

## 2. Theoretical and numerical considerations

### 2.1. Gas fraction $\alpha$

4

Table 3: Constants of Equation (3) for $\alpha_3$ and $\alpha_4$, computed with a nozzle diameter of 0.0127 m ([22, 23]).

| | $c_1$ | $c_2$ | $c_3$ | $z_0$ | $\beta$ | $\gamma$ | $\delta$ |
|---|---|---|---|---|---|---|---|
| $\alpha_3$ | 29.8785 | 0.0934 | 1.2114 | 0.016 | $-0.218$ | $-0.993$ | 0.48 |
| $\alpha_4$ | 52.9798 | 0.0781 | 1.4405 | 0.0141 | $-0.094$ | $-0.94$ | 0.51 |

The literature contains various derivations of the gas voidage distribution. However, to the best of the authors' knowledge, a comparison of the main formulas ([7, 8, 10, 14]) is not available.

Sahai and Guthrie [7] defined the gas fraction as a constant $\alpha_1'$ (see Table 2), equal to the average gas fraction in the whole plume, while in [8], $\alpha_2'$ is a function of the vertical coordinate $z$ through $r_c$ (Table 2). The additional term in the top part of the fraction is derived from the so-called drift-flux model, [6]. It is possible to define $\alpha_2'$ analytically, as a solution of a $2^{\text{nd}}$-order polynomial, leading to a closed-form formula for $z \geq z_C$, where $z_C = \frac{1}{\tan(\theta)} \left( \sqrt{\frac{4Q}{\pi U_S (\frac{U_P}{U_S}+1)^2}} \right) - a$. One can however extend the definition to the small heights. Furthermore, it is possible to redefine $\alpha_1'$ and $\alpha_2'$ such that they depend naturally on the plume radius. Indeed, the distinction between the gas-liquid mixture and the liquid is moved from the definition of the density $\rho$ to the gas fraction. This simplifies the fluid density (see next section). All in all, we define:

$$\alpha_1(r, z) = \begin{cases} \alpha_1' & \text{if } r \leq r_c(z), \\ 0 & \text{if } r > r_c(z), \end{cases} \tag{1}$$

and:

$$\alpha_2(r, z) = \begin{cases} \frac{1}{2} \left( \frac{U_P}{U_S} + 1 \right) & \text{if } z \leq z_C \text{ and } r \leq r_c(z), \\ \frac{1}{2} \left( \left( \frac{U_P}{U_S} + 1 \right) - \sqrt{\left( \frac{U_P}{U_S} + 1 \right)^2 - \frac{4Q}{\pi r_c^2(z) U_S}} \right) & \text{if } z \geq z_C \text{ and } r \leq r_c(z), \\ 0 & \text{if } r > r_c(z). \end{cases} \tag{2}$$

To the best of our knowledge, the analytical solution (2) and the lack of definition of $\alpha_2'$ in small heights were not addressed in the literature so far. Finally, the formulas applied in [10, 14] originally come from the experimental work of Castillejos and Brimacombe [22, 23]. By assuming that the gas fraction follows a Gaussian distribution and using experimental data, the latter derived $\alpha_3$ and $\alpha_4$ in the form:

$$\alpha_i(r, z) = \begin{cases} c_1 z^\beta \exp\left[ -0.7 \left( \frac{r}{c_2 z^\delta} \right)^{2.4} \right] & \text{if } z < z_0, \\ c_3 z^\gamma \exp\left[ -0.7 \left( \frac{r}{c_2 z^\delta} \right)^{2.4} \right] & \text{if } z \geqslant z_0, \end{cases} \tag{3}$$

where $i = 3, 4$, and the constants depend on the gas flow rate, the nozzle diameter, and the densities of gas and liquid. Here, the gas fraction depends naturally on both $r$ and $z$, and is discontinuous in the height.

The parameters for the numerical application are listed in Table 2 and the corresponding values for $\alpha_3$ and $\alpha_4$ are given in Table 3. Figure 2 illustrates the isolines of the gas fraction field according to each
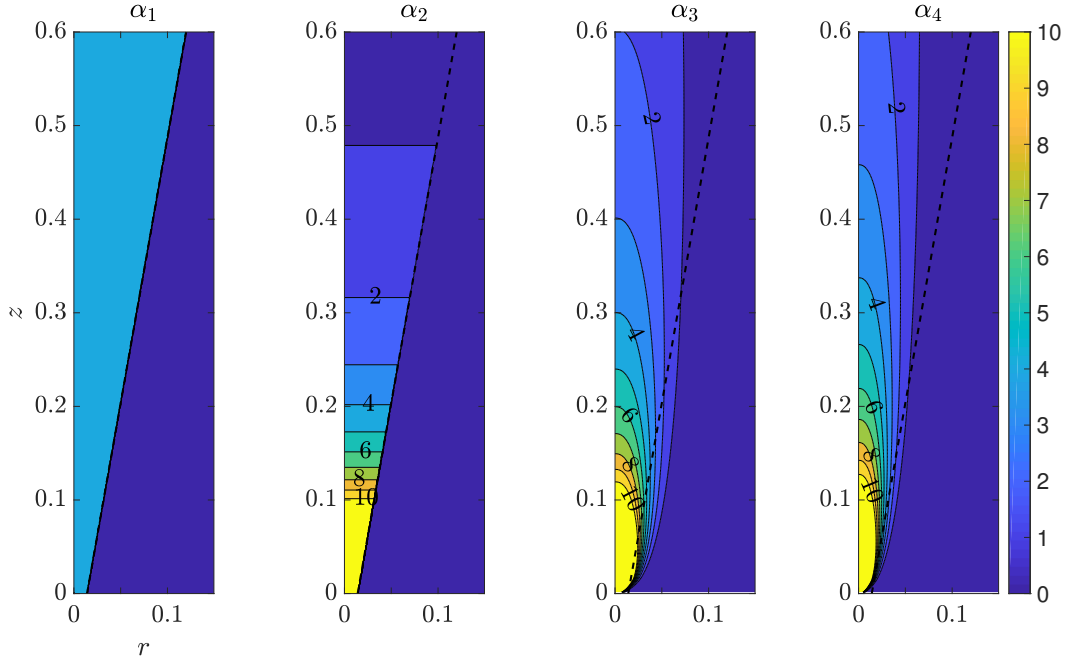
5

Figure 2: Isolines of the four different formulas for $\alpha$. The colors indicate the gas volume fraction in percentage.

definition. One can first notice that the cone $r_c(z)$ in $\alpha_1$ and $\alpha_2$ gives a sharp shape to the plume and creates a discontinuity which may be not representative of the physical reality. Thus, the plume shape is more realistic using the exponential, as in $\alpha_3$ and $\alpha_4$. It is interesting to note that the difference between the strict conical plume and the one obtained with $\alpha_3$ and $\alpha_4$ is relatively small. In most of the plume region, $\alpha$ is less than 10% with all formulas. While $\alpha_1$ is constant in the plume ($\sim 4.8\%$) and $\alpha_2$ is stratified in the height, the formulas $\alpha_3$ and $\alpha_4$ vary smoothly in both directions $r$ and $z$, which corresponds better to reality. Although $\alpha_4$ yields slightly higher values and a narrower plume than $\alpha_3$, the difference between them is negligible. Close to the nozzle, the gas fraction increases rapidly to more than 10% in the three cases $\alpha_2$, $\alpha_3$, and $\alpha_4$. While $\alpha_2$ is fixed to a constant in this region (Eq. (2)), $\alpha_3$ and $\alpha_4$ blow up at $(0,0)$, which is locally not representative of the physical reality. This preliminary discussion shows that the order of magnitude and the shape of the different gas fraction fields are not fundamentally different and that both formulas [22, 23] are very similar. In the rest of this study, only $\alpha_1$, $\alpha_2$, and $\alpha_3$ are considered.

## 2.2. Definition of the model with modified assumptions

Cylindrical ladles with one or two nozzles in the bottom are considered (see Figure 1 and Table 2). In this note, several modifications are proposed to the existing models. First, instead of using an inhomogeneous and spatially variable density $\rho$ as in the literature (e.g., $\rho = \rho_g \alpha + \rho_l(1-\alpha)$ if $r \leq r_c(z)$, and $\rho = \rho_l$ if $r \geq r_c(z)$), it is possible to simplify it to $\rho = \rho_l$ in the whole domain. Indeed, the distinction between the plume region
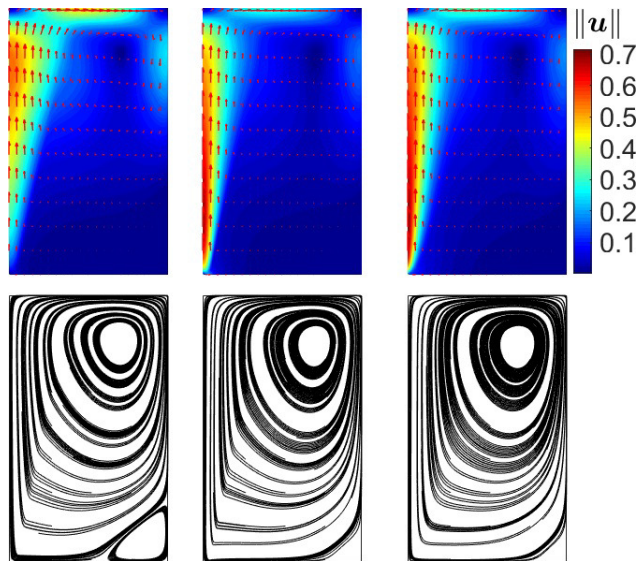
Figure 3: Axial-symmetrical configuration: Velocity field, Euclidian norm and streamlines. Left to right: $\alpha_1$, $\alpha_2$, and $\alpha_3$.

and the rest of the liquid has been introduced in the definition in the gas fractions (1) and (2). This simplification allows to use the standard incompressible Navier–Stokes equations and their numerical solver:

$$\rho_l \frac{\partial \boldsymbol{u}}{\partial t} + \rho_l(\boldsymbol{u} \cdot \nabla)\boldsymbol{u} - 2\nabla \cdot (\mu \mathbb{D}(\boldsymbol{u})) + \nabla p = (-\rho_l g + \rho_l g \alpha_i)\boldsymbol{e_z}, \quad \nabla \cdot \boldsymbol{u} = 0, \tag{4}$$

with $i = 1, 2$, or $3$. Usual boundary conditions are used, e.g., free slip with no penetration condition on the top and the left (where it is naturally imposed by the axial symmetry condition): $\boldsymbol{u} \cdot \boldsymbol{n} = 0$ and $\boldsymbol{n}^T \mathbb{S} \, \boldsymbol{t} = 0$ on $\Gamma_{\text{top}} \cup \Gamma_{\text{axis}}$, where $\boldsymbol{n}$ and $\boldsymbol{t}$ are the unit normal and tangential vectors at the boundary, and homogeneous Dirichlet on the rest of the boundary: $\boldsymbol{u} = \boldsymbol{0}$ on $\partial\Omega \setminus \{\Gamma_{\text{axis}} \cup \Gamma_{\text{top}}\}$. At $t = 0$, the fluid is assumed to be at rest in $\Omega$: $\boldsymbol{u}(0, \boldsymbol{x}) = \boldsymbol{0}$ in $\Omega$. The $k$-$\epsilon$ model ([10]) is applied to resolve the turbulence of ladle stirring ([4]).

## 3. The axial-symmetrical configuration

The models were numerically solved with the Finite Element Method (FEM), using the Taylor–Hood pair $Q_2/Q_1$ of finite elements. In other words, the velocity is approximated with continuous piecewise biquadratic functions and the pressure with continuous piecewise bilinear functions. This pair of inf-sup stable spaces is one of the most popular ones, [24]. Three meshes of the rectangular ladle (Figure 1) were applied to check the convergence of the numerical solutions. The grid sizes were $25 \times 50$, $50 \times 100$, and $100 \times 200$, corresponding to mesh sizes $h = 0.012$, $0.006$, and $0.003$ m, respectively. Finally, the time discretization scheme was an adaptive BDF2 with a maximum time step of 2 s, and $T_{\text{end}} = 60$ s. All simulations were performed with the commercial software COMSOL MULTIPHYSICS$^{\copyright}$ (version 5.3a).
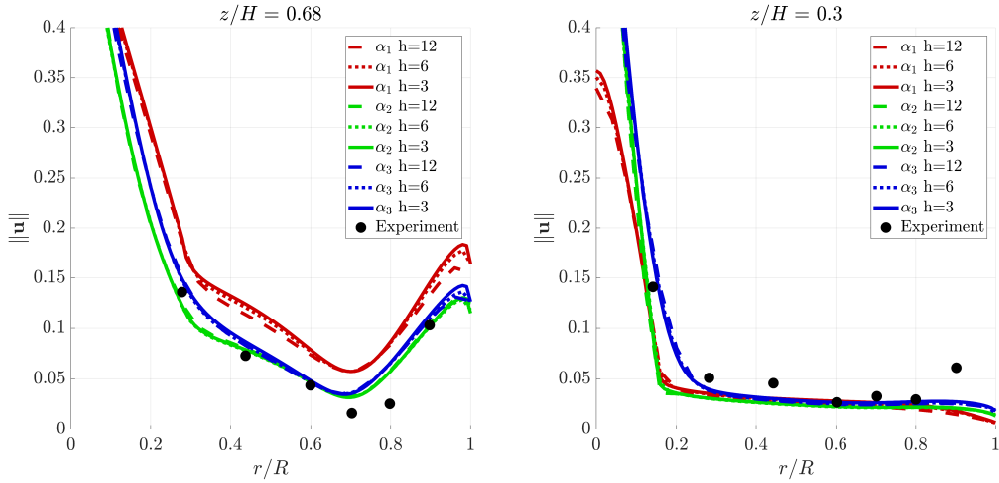
Figure 4: Axial-symmetrical configuration: Comparison of the Euclidean norm of the velocity at two different heights of the bath.

Table 4: Laboratory-scale ladle in 3d: Parameters of the ladle stirring model.

| $H$ | $R_{\text{top}}$ | $R_{\text{bot}}$ | $Q$ | $x_{n1}$ | $y_{n1}$ | $x_{n2}$ | $y_{n2}$ |
|---|---|---|---|---|---|---|---|
| 0.65 m | 0.29 m | 0.27 m | 2.83 $10^{-4}$ m$^3$/s | -0.105 m | -0.105 m | -0.105 m | 0.105 m |

The computed velocity fields on the finest mesh are displayed in Figure 3. The velocity field reveals the effect of the gas through the volume force in (4). A strong upward flow is generated close to the left boundary. Its intensity close to the nozzle is higher with $\alpha_2$ and $\alpha_3$ than with $\alpha_1$, which can clearly be assigned to the higher gas fraction in this zone (Figure 2). On the other hand, on the top left side of the domain, the velocity is slightly higher with $\alpha_1$ than with $\alpha_2$ and $\alpha_3$. In a similar way, this is due to the higher gas fraction for $\alpha_1$ ($\sim 4.8\%$) in comparison with the two others ($< 2\%$). Far from the left boundary, the velocity fields obtained with the three gas fractions are relatively similar, in the sense that they all produce one vortex located in the upper right region.

A comparison of the velocity magnitude with experimental measurements from [10] at two different heights is given in Figure 4. Similar velocity profiles are observed for all proposals of the gas fraction, but with slight differences in the amplitude. The gas fractions $\alpha_2$ and $\alpha_3$ match better with the experimental measurements than $\alpha_1$, especially in the upper region of the domain ($z/H = 0.68$).

## 4. Application to a real laboratory-scale ladle in 3d

In this application, the geometry corresponds to a real laboratory-scale water ladle with two eccentric nozzles, [20], and is described in a Cartesian space frame. Table 4 lists the parameters for this application.
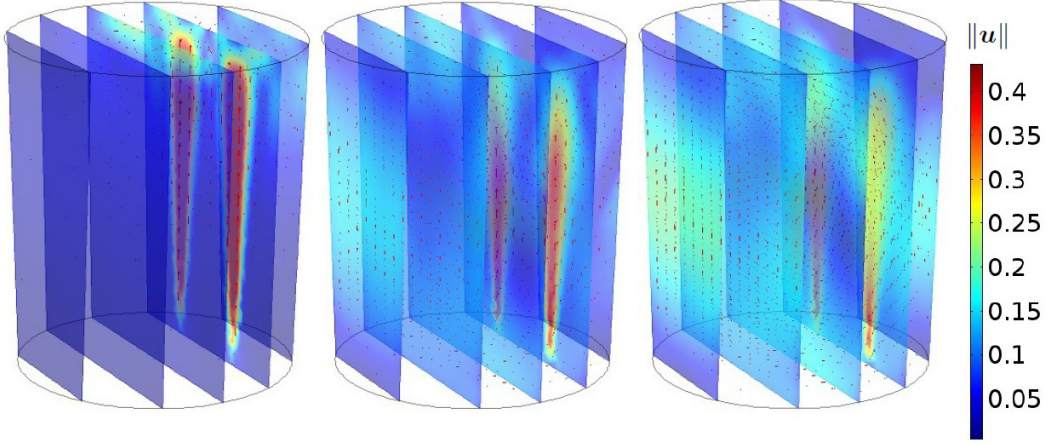
Figure 5: Velocity field magnitude $\|\boldsymbol{u}\|$ of the 3d ladle at $t = 2, 25$, and 200 s. The steady-state is reached at around 150 s.

Given the previous results, any of the gas fractions $\alpha_2$ and $\alpha_3$ can be used. However, preliminary tests have shown some convergence difficulty due, on the one hand, to the discontinuous plume shape in Eq. (2), and, on the other hand, to the blow-up of Eq. (3) at the origin. It is possible define a smoother version of $\alpha_2$ for 3d applications, which is also more realistic from the physical point of view:

$$\alpha_{ni}(x,y,z) = \begin{cases} \frac{1}{2}\left(\frac{U_P}{U_S} + 1\right)\exp\left(-b\left(\frac{(x-x_{ni})^2+(y-y_{ni})^2}{r_c(z)^2}\right)^2\right), & \text{if } z \leq z_C, \\ \frac{1}{2}\left(\left(\frac{U_P}{U_S}+1\right) - \sqrt{\left(\frac{U_P}{U_S}+1\right)^2 - \frac{4Q}{\pi r_c^2(z)U_S}}\right)\exp\left(-b\left(\frac{(x-x_{ni})^2+(y-y_{ni})^2}{r_c(z)^2}\right)^2\right), & \text{if } z \geq z_C, \end{cases}$$

where $(x_{ni}, y_{ni})$ is the center of nozzle $i = 1, 2$. The volume force in this case is defined as the sum of the buoyancy of both gas plumes, i.e., $(-\rho g + (\alpha_{n1} + \alpha_{n2})\rho g)\ \boldsymbol{e_z}$. The smoothness of the transition between the gas plume and the liquid can be set with the parameter $b$, e.g., $b = 2$.

The velocity field at $t = 2$, 25, and 200 s is illustrated in Figure 5. As expected, the volume force produces the desired gas plume effect: an upward flow is generated from the position of the nozzles at the bottom to the top surface. Its intensity decreases from the bottom, close to the nozzle, to the top, while its radius expands with $z$. This flow pattern is qualitatively similar to the ones reported in [4].

Figure 6 compares the computed velocity magnitude at the central line of one of the gas plumes from bottom to top with experimental measurements conducted in [20]. The velocity profile is similar to the observations from [4]: starting at a high value close to the nozzle (jet zone dominated by the kinetic energy of the gas), it slowly decreases a few decimeters above the nozzle and remains constant in most of the bath height (plume zone dominated by the buoyancy energy). The decrease close to the surface is due to the boundary condition. All in all, the velocity computed at the center of the gas plume is in reasonable agreement with experimental measurements.
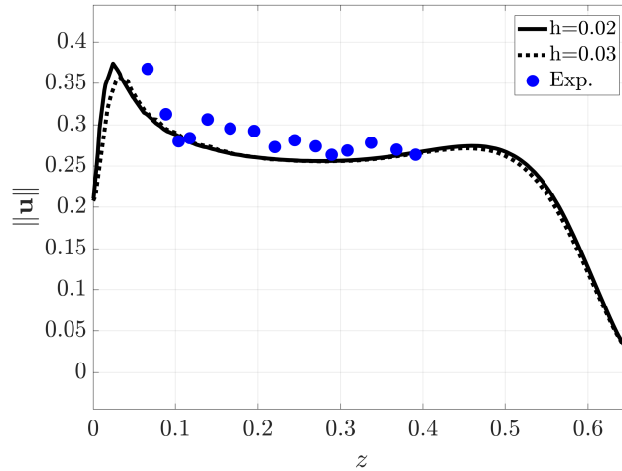
Figure 6: Laboratory-scale ladle in 3d: Euclidean norm of the velocity in the centerline of the gas plume generated by nozzle 1 (i.e., along the vertical line going from $(x_{n1}, y_{n1}, 0)$ to $(x_{n1}, y_{n1}, 0.65)$) compared with experimental measurements in [20].

## 5. Conclusions

In this note, a modified single-phase model for ladle stirring was derived from existing 'quasi-single phase' models. Some changes in the modeling assumptions were introduced to allow a more straightforward implementation in standard incompressible flow solvers. The shapes of the gas fraction were clarified. Although the clarification showed that their order of magnitude and their shape are quite similar, some differences are still observable: the formula $\alpha_1$ ([7]) produces higher gas fractions in the top region of the ladle than $\alpha_2$ and $\alpha_3$ ([8, 22]). This is reflected in the numerical results: in the first case, the computed velocity magnitude is higher than the experimental data, while the two other formulas give reasonable agreement. They can thus be equivalently used. Subsequently, the gas fraction $\alpha_2$ was applied for a real laboratory-scale 3d ladle with two eccentric nozzles. The simulation results showed that the velocity profile in the bath corresponds with results from the literature and the velocity at the centerline of the plume is in a relative good agreement with experimental data. In summary, we conclude that the accuracy of the results computed with the present single-phase model using $\alpha_2$ (Eq. (2)) or $\alpha_3$ (Eq. (3)) is sufficient for employing it as an efficient model in simulations of optimal flow control problems.

## References

[1] L. Sirovich, Turbulence and the dynamics of coherent structures. I. Coherent structures, Quart. Appl. Math. 45 (3) (1987) 561–571.

[2] B. R. Noack, M. Morzynski, G. Tadmor, Reduced-Order Modelling for Flow Control, Vol. 528, Springer Verlag, 2011.

[3] A. Caiazzo, T. Iliescu, V. John, S. Schyschlowa, A numerical investigation of velocity-pressure reduced order models for incompressible flows, J. Comput. Phys. 259 (2014) 598–616.

[4] D. Mazumdar, R. I. L. Guthrie, The physical and mathematical modeling of gas stirred ladle systems, ISIJ Intern. 35 (1) (1995) 1–20.

[5] R. Debroy, A. K. Majumdar, D. B. Spalding, Numerical prediction of recirculation flows with free convection encountered in gas-agitated reactors, App. Math. Model. 2 (3) (1978) 146–150.

[6] J. H. Grevet, J. Szekely, N. El-Kaddah, An experimental and theoretical study of gas bubble driven circulation systems, Intern. J. of Heat and Mass Transf. 25 (4) (1982) 487–497.

[7] Y. Sahai, R. I. L. Guthrie, Hydrodynamics of gas stirred melts: Part II. Axisymmetric flows, Metall. Trans. 13 (2B) (1982) 203–211.

[8] D. Balaji, D. Mazumdar, Numerical computation of flow phenomena in gas-stirred ladle svstems, Steel Res. 62 (1) (1991) 16–23.

[9] D. Mazumdar, J. W. Evans, Modeling of steelmaking processes, CRC Press, 2009.

[10] J. S. Woo, J. Szekely, A. H. Castillejos, J. K. Brimacombe, A study on the mathematical modeling of turbulent recirculating flows in gas-stirred ladles, Metall. Trans. 21 (21B) (1990) 269–277.

[11] R. Bernard., R. S. Maier, H. T. Falvey, A simple computational model for bubble plumes, App. Math. Model. 24 (3) (2000) 215–233.

[12] D. Mazumdar, T. Narayan, P. Bansal, Mathematical modelling of mass transfer rates between solid and liquid in high-temperature gas-stirred melts, App. Math. Model. 16 (5) (1992) 255–262.

[13] S. Ganguly, S. Chakraborty, Numerical investigation on role of bottom gas stirring in controlling thermal stratification in steel ladles, ISIJ Intern. 44 (3) (2004) 537–546.

[14] A. Mukhopadhyay, P. Deb, A. Ghosh, B. Basu, R. Dutta, P. Kumar, Prediction of temperature in secondary steelmaking : mathematical modelling of fluid flow and heat transfer in gas purged ladle, Steel Res. 72 (5) (2001) 192–199.

[15] M.-Y. Zhu, I. Sawada, N. Yamasaki, T.-C. Hsiao, Numerical simulation of three-dimensional fluid flow and mixing process in gas-stirred ladles, ISIJ Inter. 36 (5) (1996) 503–511.

[16] M. Goldschmit, A. C. Owen, Numerical modelling of gas stirred ladles, Ironmak. and Steelmak. 28 (4) (2001) 337–340.

[17] D. Mazumdar, R. I. L. Guthrie, A Comparison of three mathematical modeling procedures for simulating fluid flow phenomena in bubble-stirred ladles, Metallurgical and Materials Transactions B 25 (2) (1994) 308–312.

[18] D. Mazumdar, R. I. L. Guthrie, On the numerical computation of turbulent fluid flow in CAS steelmaking operations, App. Math. Model. 19 (9) (1995) 519–524.

[19] M. P. Schwarz, Simulation of gas injection into liquid melts, App. Math. Model. 20 (1) (1996) 41–51.

[20] T. Palovaara, V.-V. Visuri, T. Fabritius, Physical modelling of gas injection in a ladle, in: Proceedings of the 7th International Congress on Science and Technology of Steelmaking, 2018.

[21] D. Mazumdar, R. I. L. Guthrie, Y. Sahai, On mathematical models and numerical solutions of gas stirred ladle systems, App. Math. Model. 17 (5) (1993) 255–262.

[22] A. H. Castillejos, J. K. Brimacombe, Measurements of physical characteristics of bubbles in gas-liquid plumes: Part ii. local properties of turbulent air-water plumes in vertically injected jets, Metall. Trans. 18B (1987) 595–601.

[23] A. H. Castillejos, J. K. Brimacombe, Physical characteristics of gas jets injected vertically upward into liquid metal, Metall. Trans. 20B (5) (1989) 595–601.

[24] V. John, Finite element methods for incompressible flow problems, Vol. 51 of Springer Series in Computational Mathematics, Springer, Cham, 2016.